Facile Creating a Hierarchical and Hydrophobic Fe-Co/LZSM-5 Catalyst for the Oxidative Desulfurization Process

Lisa Adhani[1,2], Bambang Heru Susanto[1], and Mohammad Nasikin[1*]

[1]*Department of Chemical Engineering, Faculty of Engineering, Universitas Indonesia, Jl. Dr. Indro S, Depok 16424, Indonesia*

[2]*Department of Chemical Engineering, Faculty of Engineering, Universitas Bhayangkara Jakarta Raya, Jl. Harsono RM No. 67, Jakarta Selatan 12550, Indonesia*

* ***Corresponding author:***

email: mnasikin@che.ui.ac.id

Received: April 1, 2024
Accepted: May 20, 2024

DOI: 10.22146/ijc.95267

Abstract: *This research involved top-down dealumination and steam treatment methods to design the hierarchical pores of ZSM-5, which is then wet-impregnated with a Fe-Co. This method overcomes the steric barrier that hinders the oxidative desulfurization (ODS) process and makes the catalyst hydrophobic, thereby allowing it to overcome the biphasic hindrance caused by the difference in polarity between the fuel oil and the oxidant. Characterization of the catalyst's properties based on BET and BJH, XRF, and contact angle, as well as testing its performance on DBT model oil in* n-*hexadecane and Indonesian commercial diesel were conducted. Simulation of the reaction energy profile using density functional theory calculations was also carried out to deepen insight into the mechanism of the reaction. Results of this study show that the catalyst has excellent catalytic reactivity in the long-chain hydrocarbon ODS process, with a TOF number of 183* h^{-1}.

Keywords: *hierarchical; hydrophobic; biphasic; steric; dealumination*

■ INTRODUCTION

Sulfur is a major source of transportation fuel pollution. The process of burning fuel containing sulfur will cause the formation of sulfur oxide (SO_x), which is toxic, corrosive, and harmful to the ecosystem. Therefore, the European Union issued strict environmental rules and regulations to put great pressure on refinery operations to produce fuel with the lowest sulfur content [1].

Desulfurization of fuels to very low levels is increasingly necessary today, not only because of increasing concerns about environmental and legal requirements but also because very low sulfur fuels are a key requirement in fuel cell applications. Currently, fuel sulfur content requirements are increasingly stringent to achieve net zero emissions. Refineries around the world continue to develop new processes to reduce sulfur levels in fuel. Therefore, researchers are trying to find an effective process. Nowadays, it is widely known that oxidative desulfurization (ODS) is considered a new technology to achieve deep desulfurization [2]. The biggest advantage of the ODS process is a low reaction temperature and pressure. Previous ODS research has used various types of oxidants, including hydrogen peroxide (H_2O_2), *t*-butylhydroperoxide (TBHP), air, molecular oxygen, and ionic liquids to increase oxidative activity. H_2O_2 is recognized as superior as an oxidant, and the best results are achieved when utilizing H_2O_2 with a heterogeneous catalyst. Transition metals such as Fe, Cu, Ti, Co, and Cr are intensively studied in the oxidation of organosulfur compounds [2-3]. Transition metals with ferromagnetic properties are preferred because they can overcome resonance in organosulfur compounds, facilitating the ODS process, which involves electron transfer [4-5].

However, the search for catalysts is currently being carried out to overcome four problems in the ODS process, namely (i) biphasic hindrance, that is, layers caused by the polarity of the oxidant and the non-polar of the fuel oil, (ii) steric barrier caused by the large size of the organosulfur contained in the fuel, (iii) excessive use of oxidants, which causes problems in the by-product

separation process and fuel quality, and (iv) sulfone separation process, which results from the organosulfur oxidation process in fuel [2].

Currently, zeolite or ZSM-5 is attracting the attention of many researchers to obtain ultra-low sulfur diesel (ULSD) from the oxidative desulfurization process because of the high selectivity of its framework properties. The adsorption properties of the framework catalyst make it easier to separate the results of the ODS process and do not require a process for purification [6]. However, the pore size of ZSM-5 is dominated by 5 Å, and this makes the steric barrier a problem because the size of the organosulfur molecules in the fuel is more than 5 Å, especially dibenzothiophene (DBT). Many reports began to be made about zeolite engineering for the success of the ODS process [7-9].

Wang et al. [6] carried out synthetic engineering of hierarchical ZSM-5, which is amphiphilic, using the bottom-up method, namely a synthetic method from scratch and impregnated with Ti. However, the bottom-up synthesis process of ZSM-5 is still not able to achieve this characterization. Zhu et al. [10] carry out Y-zeolite dealumination to form a hierarchical zeolite with tri-coordinate aluminium. However, it is still a challenge for the tri-coordinate aluminum process, which is bound by the dealumination results. Jafarinasab et al. [11-12] inserted Co into zeolitic imidazolate framework-67 to form CoZIF-67, which was then modified again with a combination of encapsulating HPMo into CoZIF-67 [11-12]. It became a challenge in the bottom-up synthesis of ZIF, which binds to metal Co to form a metal-organic framework and encapsulate HPMo. Wang et al. [9] made cheese-like hierarchical pores that modified C-ZSM-5 as a Ti support, where ZSM-5 was synthesized bottom-up [9]. Dashtpeyma et al. [13] modified zeolite clinoptilolite with $BiVO_4$-CuO but its performance still used the mass transfer agent of acetonitrile.

Zhang et al. [14] carried out micro-mesopore engineering on zeolite, which they synthesized bottom-up and then impregnated with Ti induced in amide to form $Ti(OH_2)_2(OH)_2(OSi)_2$. This was done because it was considered that the Ti contained in the reported zeolites was commonly not well distributed, and conventionally, this was quite difficult. So, the Ti that is induced in the amide becomes $Ti(OH_2)_2(OH)_2(OSi)_2$, making Ti more easily distributed in zeolite or ZSM-5 [14]. However, the process for obtaining the Ti-amide compound is not explained clearly. Jangi et al. [4] said that using natural zeolite can reduce costs in the synthesis process using ODS catalysts. Therefore, they carried out an impregnation process using phosphotungstic acid (PTA) into natural zeolite. This type of ferrite is obtained by reacting ammonium form ferrite with natural zeolite to PTA-Fer/Zeolite [4]. However, the ODS process still uses mass transfer agents, extraction processes in the result separation process, and oxidants that exceed the stoichiometry. Currently, there are many studies that seek to obtain catalysts that can overcome problems in the ODS process and increase its effectiveness in facile synthesis, selectivity, and performance. The desired catalyst has hierarchical pores to increase reaction transport, is mesopore to facilitate the oxidation reaction of DBT with a large molecular size, about 9 Å [5,14], and is hydrophobic to overcome biphasic hindrance [9-10].

This study implemented a hierarchical pore engineering strategy through top-down dealumination of the LudoxZSM-5 (starting now referred to as LZ) catalyst, supporting the Fe-Co ferromagnetic transition metal. The resulting catalyst Fe-Co/LudoxZSM-5Hierarchy (Fe-Co/LZ-H) demonstrated a unique dominance of mesoporosity and hydrophobicity, which was not previously reported. LZ is ZSM-5, which was synthesized with a Si source from Ludox chemical. Subsequently, a catalyst effectiveness test was conducted on DBT model diesel fuel dissolved in the long-chain hydrocarbon compound hexadecane, which has not been found in ODS process catalyst test reports. A catalyst performance test was also carried out on the Indonesian commercial diesel ODS process, which is rarely reported. The profound reasons underlying the extraordinary catalytic activity of the Fe-Co species impregnated on LZ-H are explained by density functional theory (DFT) calculations in reaction energy profile studies. The catalyst obtained has excellent potential to be produced and applied in fuel desulfurization processes and promises good prospects in

catalyst engineering.

■ EXPERIMENTAL SECTION

Materials

LZ is ZSM-5, which is synthesized with its silica source from Ludox, and this LZ is obtained from the synthesis results of the Chemistry laboratory of the Institut Teknologi Bandung, Indonesia. HF, $Co(NO_3)_2{\cdot}6H_2O$, $Fe(NO_3)_3{\cdot}9H_2O$, NH_4Cl, DBT, *n*-hexadecane, H_2O_2, and $AgNO_3$ were obtained from Merck Indonesia (all analytical pure materials without purification process). Aquadest and DBT model oil in *n*-hexadecane, as well as Indonesian commercial diesel were also used in this study.

Instrumentation

The instrument used for catalyst characterization is a surface area analyzer (SAA, Quantachrome Nova 4200e) with the Brunauer Emmett-Teller (BET) and Barret-Joiner-Halenda (BJH) methods to measure the N_2 adsorption-desorption isotherm and determine the surface area, pore volume, and diameter pore. X-ray fluorescence (XRF, ED-XRF type, Rigaku NexCG) to determine metal content. UV-vis spectrophotometer (Thermo Scientific Genesys 10S Spectrum) was used to measure the sulfur conversion. To measure the water contact angle and to drip demineralized water on the catalyst surface, the water droplets are recorded with a digital camera, and the contact angle is determined from the digital image of the water droplets on the catalyst surface [6,15].

Procedure

Hierarchical process

Hierarchy is carried out using a top-down dealumination method, namely treatment, to create a hierarchical system in ZSM-5 through post-treatment procedures using acid and steam treatment. That is by mixing 100 g of LZSM-5 with 600 mL of 10% HF and stirring at 65 °C for 25 min. Next, it is filtered and cooled to room temperature, then washed with distilled water until the pH is neutral. Steam treatment was carried out with NH_4Cl for 5 h at 90 °C, washed until free of Cl^-, and dried at 100 °C for 8 h. Finally, the result was calcined for 3 h at 550 °C in a furnace [16-17], so a LZ-H was obtained.

Impregnation bimetal Fe-Co

Bimetal Fe-Co impregnation on LZ-H was carried out using the wet impregnation method. The concentration of Fe and Co metals used is 10% of the catalyst with a Fe:Co ratio of 2:1. $Fe(NO_3)_3{\cdot}9H_2O$ and $Co(NO_3)_2{\cdot}6H_2O$ in aquadest were prepared separately. Then, the sample of hierarchical ZSM-5 was added and immersed in a solution of $Fe(NO_3)_3$ and $Co(NO_3)_2$. The mixture was stirred for 3 h at room temperature, dried at 60 °C for 12 h, and calcined at 450 °C for 5 h [18]. The LZ-H catalyst embedded with Fe-Co is obtained and coded as Fe-Co/LZ-H.

ODS catalytic

The ODS process was carried out in a 3-neck round bottom flask with a magnetic stirrer and reflux column. The catalyst was put into the flask, 30% H_2O_2 was added as an oxidant, and then 10 mL of fuel was added. The operation is carried out on a bath with a stable temperature while stirring with a magnetic stirrer at atmospheric pressure. The study for optimum conditions was tested by studying the effect of operating condition parameters, which included the amount of catalyst using Fe-Co/LZ-H as the catalyst dose used, i.e., 0.5, 1, 2, and 3% (w/v) of 10 mL DBT model oil in *n*-hexadecane at a concentration of 500 ppm, the amount of oxidant according to the [O]/[S] ratio is 1, 2, 4, and 7, temperature of 30, 45, and 60 °C, as well as the reaction time of 30, 45, and 60 min. Then, temperature, oxidant ratio, time, and optimum operating conditions were applied to the LZ and LZ-H catalysts. Finally, it was also applied to the Fe-Co/LZ-H catalyst for commercial diesel.

The amount of sulfur converted was determined using UV-vis, calibrated for absorbance, and a measured concentration series search was carried out at a wavelength of 320 nm. Catalyst effectiveness is recorded as DBT conversion using the Eq. (1) [19-20];

$$\text{DBT conversion } (\alpha) = \frac{C_0 - C_i}{C_0} \times 100\% \quad (1)$$

where C_0 is the initial concentration of DBT, C_i is the final concentration of DBT, and α is DBT conversion.

Then, in the catalytic reaction, the turnover frequency (TOF) of sulfide oxidation is calculated as Eq. (2) [14];

$$TOF = \frac{n(sulfide)_{initial} \times \alpha}{n(Fe-Co) \times reaction\ time} \quad (2)$$

where n(sulfide)initial is the initial mole of sulfide, α is DBT conversion, and n(Fe-Co) is the mole of Fe-Co species in the catalyst.

DFT calculations to see the energy profile of the ODS process

DFT calculation to view the energy profile was carried out with Gaussian09 software [14] with a model structure, and the Fe-Co/LZ-H structure is a crystallographic information file (CIF) resulting from the results of the Rietveld refinement process. DFT was carried out using the functional B3LYP method, with a basis set for the chemical properties of the 6-31G+(d,p). Complete simulations were conducted with optimization and frequency (opt+freq) [21].

■ RESULTS AND DISCUSSION

Catalyst Characterization

BET results show that the LZ-H catalyst design with a dealumination strategy with HF causes changes in surface catalyst characteristics (Table 1). However, the catalyst generally has a large surface area under the general properties of zeolites. Table 1 shows that the hierarchical process used dealumination treatment with steam treatment succeeded in increasing the surface area from 264.35 to 299.74 $m^2\ g^{-1}$ and the number of mesopores from 0.03701 to 0.05897 cc g^{-1}. This then maintains a high surface area after impregnation, which is 271.93 $m^2\ g^{-1}$, with the formation of multimodal pores, so it can be said that the hierarchy is successful when there are several pore sizes without eliminating micropores [22].

Table 1 shows a less significant increase in the average pore radius after dealumination and impregnation treatments. In a more general context, if the radius of a pore is enlarged, the volume of the pore tends to increase [23]. This is because pore volume is usually related to the amount of space available within it, with increasing pore radius causing more space to be available. However, material phenomena and structural changes can be complex in various contexts, such as geometric restrictions due to the limited zeolite structure, which limits the increase in pore volume as the pore radius increases. The zeolite structure can sometimes become unstable when the pore radius becomes very large. At this point, the zeolite structure can begin to collapse or degrade, which can ultimately reduce the adequate pore volume, or pore stretching can occur, which causes an increase in pore volume without an increase in pore radius. Metal loading in zeolite also has a complex effect depending on the stability/thickness of the pores and the radius ionic [24]. Table 1 shows that after dealumination, there was a slight increase in the average pore radius and volume, which may be due to changes in the pores in which severe punishment of micropores to form mesopores. Then, after the bimetal Fe-Co impregnation treatment, there was a slight increase in the average pore radius. Still, the pore volume decreased compared to after the bimetal Fe-Co impregnation treatment. There was a slight increase in the average pore radius, but the pore volume decreased compared to before. Bimetal Fe-Co can be used as a connectivity controller, which is visible in pore connectivity where Fe-Co impregnation on LZ-H causes changes in surface area, pore radius, pore volume, and pore distribution [25]. Apart from that, Fe-Co also causes the reappearance of micropores without weakening the mesopores (Table 1).

Table 1. Physicochemical properties of LZ, LZ-H, and Fe-Co/LZ-H

Catalyst	[a]Surface area ($m^2\ g^{-1}$)	[b]Pore radius average (nm)	[b]Micropore volume (cc g^{-1})	[b]Mesopore volume (cc g^{-1})	[b]Macropore volume (cc g^{-1})
LZ	264,35	0.32139	0.00218	0.03701	0.00455
LZ-H	299.74	0.33293	0.00000	0.05897	0.00092
Fe-Co/LZ-H	271.93	0.33493	0.00293	0.04520	0.00069

[a]determined by BET
[b]determined by BJH

So it can be said that this catalyst design succeeded in increasing the number of meso and hierarchical pores to overcome the steric barrier problem in the ODS process, where it is known that the organosulfur in the fuel is more than 5 Å in size, especially DBT, which is in larger quantities, and this has been a problem in the ODS process so far [2,7]. Hierarchical catalytic pores offer the potential to (i) reduce steric constraints to overcome the diffusion of large molecules, (ii) increase the rate of intercrystalline diffusion, (iii) maximize catalyst utilization, and (iv) modulate selectivity towards the target product [26].

Adsorption-desorption of N_2 on the catalyst using BET analysis is depicted in Fig. 1, which exhibited that all catalysts are porous solids, under the zeolite characterization. The general tendency of the adsorption-desorption curve shows a type IV profile for mesoporous solids, where adsorption at low P/P_0 associated with the filling of smaller pores increases slowly around $P/P_0 > 0.2$ so that the curve slopes gently and there is a sharp increase when P/P_0 0.9 to close to 1 [22,27]. The difference between adsorption and desorption causes a hysteresis loop due to capillary condensation. In the curve, there is a hysteresis loop at low pressure, and the largest loop is found in Fe-Co/LZ-H. This is due to the presence of small micropores and mesopores. Small pore connectivity can be seen in LZ-H and Fe-Co/LZ-H, indicating that most of them are flakes with non-rigid aggregates and have an ink bottle effect. This is why when reducing the pressure during desorption, molecules with lower energy tend to require a higher chemical potential gradient to pull the adsorption molecules out of the pore so that the hysteresis loop in the low-pressure region is larger [28-29].

The number of mesopores can also be seen from the distribution curve in Fig. 2, where you can see that pores are distributed in mesopores with high intensity in LZ-H. Still, the number of micropores disappears according to the size of the BJH pores and reappears in Fe-Co/LZ-H, namely hierarchical LZ impregnated with bimetal Fe-Co (Table 1). So, the resulting catalyst has hierarchical pores according to the agreed provisions. The hierarchy is said to be successful if a large pore size is achieved without removing the micropores [22]. Pore size classification is carried out using BJH analysis following IUPAC provisions, namely < 2 nm for micropore size, 2–50 nm for mesopore, and macropore size > 50 nm [30]. Fig. 2 shows that the Fe-Co/LZ-H catalyst is a catalyst with multimodal micro/meso/macropores and distribution pores of 1 to 70 nm. The pore distribution depicted in Fig. 2 is the pore width versus the incremental pore profile. The incremental pore size distribution analysis method was used due to the addition of mesopores and multimodal pores. According to Liu et al. [31], the presentation of distribution analysis is very important because it will determine the interpretation of the data. The presentation of pore distribution with incremental pore is very dependent on experimental data on point

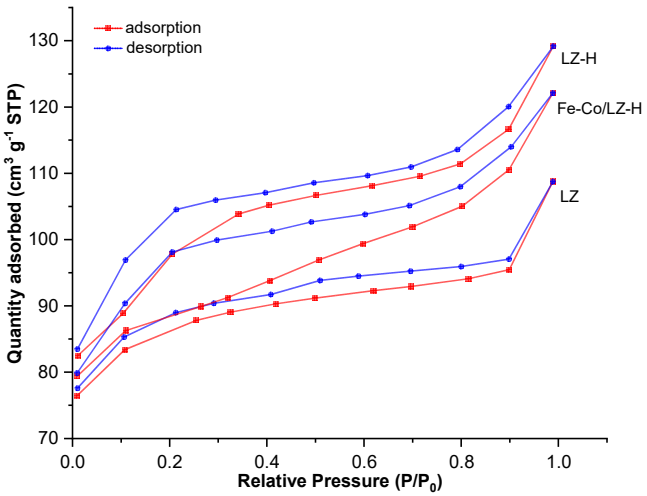

Fig 1. Nitrogen adsorption-desorption isotherms

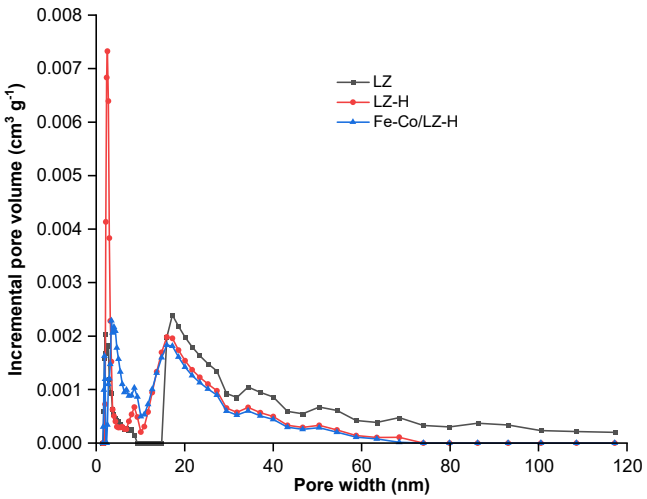

Fig 2. The pore distribution of pore width versus incremental pore

distances/intervals. The addition of mesopores causes the pores to be more distributed at the pore size point of 20–30 nm. The pore distribution profile in Fig. 2 shows that the catalyst pores are arranged regularly [32]. ZSM-5 is generally known to have a regular structure [33]. In zeolites with hierarchical pores, a wide distribution of peaks will be seen, indicating the presence of pores of various sizes [27,32], as shown by the distribution profile in Fig. 2.

In Scheme 1, a hierarchical process using a top-down dealumination method together with steam processing is used. The dealumination process involves the use of HF to extract Si from the ZSM-5 framework. Steam treatment with NH_4Cl helps accelerate the formation of hydroxyl or silanol as a recovery resulting from the breaking of Al–O bonds by HF. Steam treatment, in turn, facilitates optimal Si migration to specific hydroxyl sites, preventing massive structural collapse of the framework. After steam processing, the hydroxyls of the broken Al–O bonds remain intact, thereby reducing the possibility of framework damage and maintaining pore connectivity [17]. The BET instrument will provide further information regarding pore connectivity.

The Si/Al ratio analysis of the XRF test results listed in Table 2 increases on the Fe-Co/LZ-H catalyst, i.e. 51.78. This is because the dealumination process removes some of the Al elements in the catalyst framework structure, which creates new space and results in increasing the Si shown in Scheme 1 [34]. Impregnation is not the cause of the high Si/Al ratio, but it can be said that impregnation still maintains the high Si/Al ratio value. Then the study of analysis of the catalyst elements using XRF (Table 2) shows that Fe-Co with a ratio of 2:1 was successfully embedded in the LZ-H support, which is read in its oxide form, namely Fe_2O_3 1.5% and CoO 0.7%.

From Table 2, it can also be seen that Fe-Co/LZ-H has a Si/Al ratio of 51.78. Increasing the Si/Al ratio alters the catalyst's surface properties, making it more hydrophobic [35], and silica is widely used as an ingredient to make hydrophobic materials [36].

Table 2. Elemental composition in catalysts based on XRF analysis

Catalyst	Si/Al ratio	Fe-Co content in oxide (%)	
		Fe_2O_3	CoO
LZ	15.00	0.0	0.0
LZ-H	-	-	-
Fe-Co/LZ-H	51.78	1.5	0.7

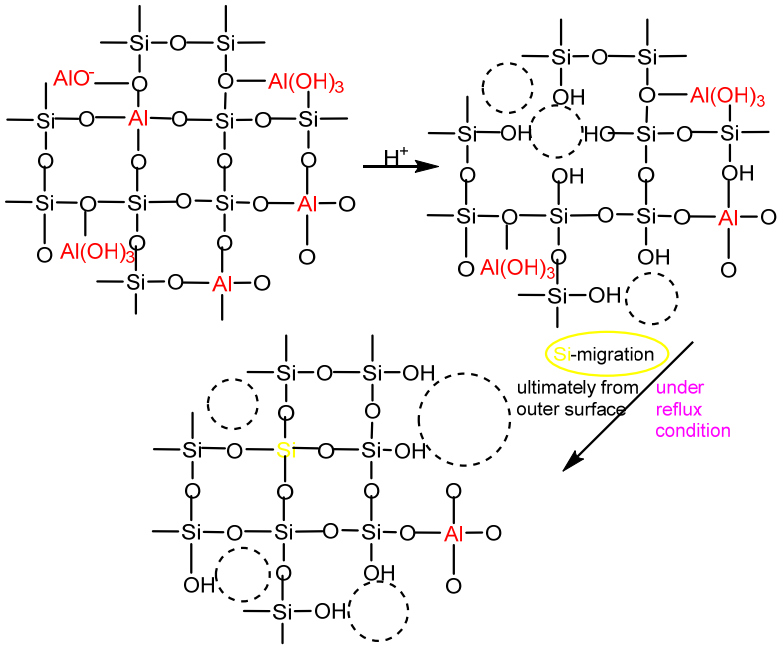

Scheme 1. Hierarchical process using top-down dealumination method

Alharbi et al. [37] designed a water contact angle category at the surface, as depicted in Fig. 3(a). According to the results presented in Fig. 3(b), the water contact angle observed on the surface of the Fe-Co/LZ-H catalyst is 115°. This value is within the range considered appropriate for a surface to be considered hydrophobic, which is typically between 90–150° [15]. The idea of creating a hydrophobic surface on the catalyst for the ODS process is very important because hydrophobicity is useful for overcoming the biphasic hindrance that generally occurs in the ODS process. If this problem is resolved, mass transfer agents will no longer be needed, so oxidants are effective according to their stoichiometry [10].

ODS Catalytic

Study looking for operating conditions for ODS with Fe-Co/LZ-H catalyst

The study for the conditions optimum of the ODS process with the Fe-Co/LZ-H catalyst was carried out on DBT in *n*-hexadecane as a model oil at a concentration of 500 ppm for 10 mL. This is done by varying the amount of catalyst according to the catalyst dose used, i.e., 0.5, 1, 2, and 3% (w/v), varying the ratio of oxidant to DBT concentration in the model oil ([O]/[S]) of 1, 2, 4, and 7, temperature variations of 30, 45, and 60 °C, as well as time reaction variations, i.e., 30, 45, and 60 min. The condition with maximal DBT conversion was taken as the operating condition optimum.

Effect of the amount of catalyst

The trend depicted in Fig. 4 illustrates a correlation between the amount of catalyst used as a percentage of fuel versus the resulting conversion rate. As seen, conversion rates increase with the amount of catalyst used but begin to decrease once the amount surpasses 2% (w/v). This suggests that the optimal amount of catalyst has been achieved at a dosage of 2% (w/v). At this point,

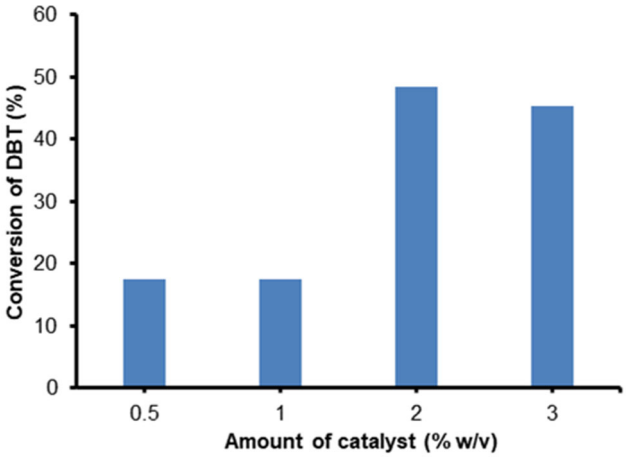

Fig 4. Effect of the amount of catalyst on Fe-Co/LZ-H catalyst performance under standard conditions: 10 mL model oil DBT in *n*-hexadecane 500 ppm, [O]/[S] = 2, T = 45 °C, for 45 min

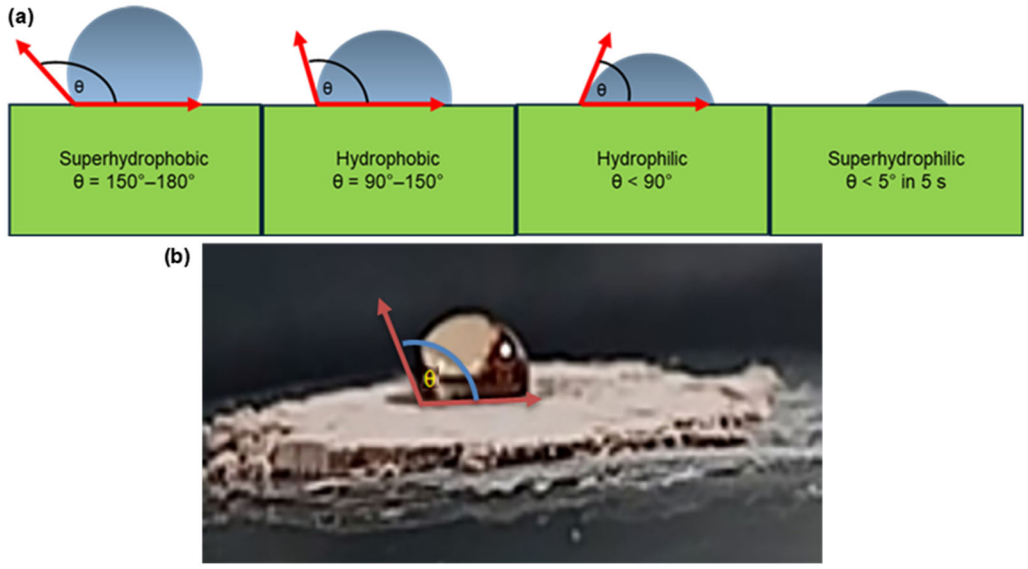

Fig 3. Water contact angle at (a) the surface and (b) Fe-Co/LZ-H catalyst (this study)

the catalyst provides ample active sites for efficient catalytic reactivity. However, if too many active sites exist, reactant collisions may become ineffective, decreasing reaction yield. Moreover, an excess of catalyst may disrupt the reaction equilibrium by competing with active species, ultimately resulting in a decline in activity [38].

Effect of ratio molar oxidant H_2O_2 and DBT ([O]/[S])

The oxidant ratio is the ratio of the amount of oxidant used to the sulfur concentration in the fuel. Fig. 5 shows that the highest conversion is at an [O]/[S] ratio of 2, meaning that here the goal has been achieved to obtain optimum conditions at an [O]/[S] ratio according to stoichiometry that is [O]/[S] = 2. The trend in Fig. 5 shows that the addition of oxidant beyond the stoichiometry has a negative effect because it will decrease the conversion significantly. This is because oxidation with oxidants produces water as a by-product. If excess water is produced, it will make it difficult for oxidant reactions to occur with species at the catalyst's active site [14]. Fig. 5 also illustrates that oxidants play a very important role in oxidation reactions under optimum conditions, which greatly impact the catalyst's reactivity. The oxidant is given to provide a certain amount of oxygen for the oxidation process, and Fe-Co is impregnated to have a significant impact in decomposing the oxidant H_2O_2 to produce abundant molecular oxygen to ensure that the organosulfur oxidation process in the fuel runs optimally. The phenomenon in Fig. 5 shows that the Fe-Co impregnation objective was achieved.

Effects of temperature

It should be remembered that the ODS process is very attractive because it can operate at mild operating conditions, much lower than the conventional HDS process [7]. Fig. 6 shows that the DBT conversion increases significantly with increasing temperature and decreases slowly after a temperature of 45 °C. This is possible because the nature of H_2O_2 is easily decomposed at high temperatures. Therefore, the oxidant may have been decomposed before contact with the active site, which will determine the outcome of the H_2O_2 decomposition reaction so that it is possible to form other reactions that interfere the oxidation reaction, resulting in a decrease in DBT conversion [14].

Effects of reaction time

The reaction time follows the reaction pattern and nature of the reaction to the factors that affect reactions, such as temperature, number of reactants, and catalysts [14,39]. In this study, the variation of the reaction time is at 30, 45, and 60 min, and Fig. 7 shows the optimum reaction in 45 min. As time increases, the conversion does not decrease significantly. In Fig. 7, the trend of the phenomenon of time influence approaches the trend of temperature influence.

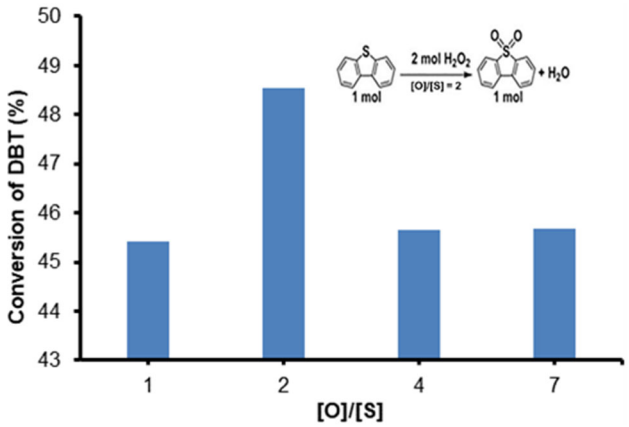

Fig 5. Effect of [O]/[S] ratio in the ODS process with Fe-Co/LZ-H catalyst, under standard conditions: 10 mL model oil DBT in *n*-hexadecane 500 ppm, amount of catalyst 2% (w/v), T = 45 °C, for 45 min

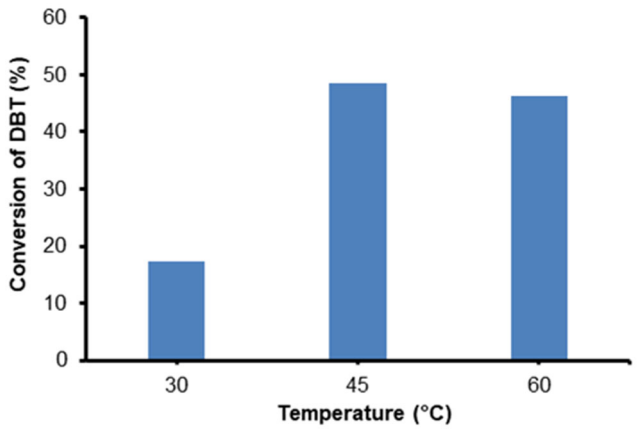

Fig 6. Effect of temperature in the ODS process with Fe-Co/LZ-H catalyst, under standard conditions: 10 mL model oil DBT in *n*-hexadecane 500 ppm, amount of catalyst 2% (w/v), [O]/[S] = 2, for 45 min

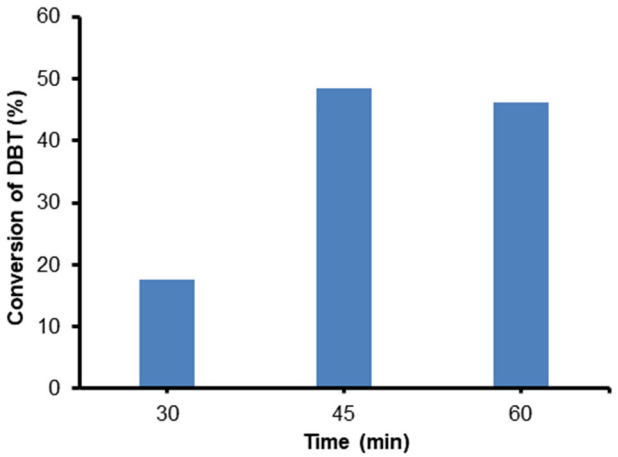

Fig 7. Effect of reaction time in the ODS process with Fe-Co/LZ-H catalyst, under standard conditions: 10 mL model oil DBT in n-hexadecane 500 ppm, amount of catalyst as dose 2% (w/v), [O]/[S] ratio of 2, and temperature 45 °C

ODS catalytic process

The effectiveness test of the LZ, LZ-H, and Fe-Co/LZ-H catalyst was carried out with model oil, that is, DBT in hexadecane with a concentration of 500 ppm and also with commercial diesel Indonesia (B30) with a sulfur concentration of 556 ppm. The ODS process was carried out under optimum conditions, i.e., at a temperature of 45 °C, a catalyst amount of 0.2 g, an [O]/[S] ratio of 2, and a reaction time of 45 min. Fig. 8. shows the DBT conversion in the oil model with a catalyst: LZ of 15.49%, LZ-H of 27.70%, and Fe-Co/LZ-H of 48.50%. The Fe-Co/LZ-H catalyst also provides good catalyst activity when oxidizing real Indonesian diesel, which can be seen in the picture as being able to convert sulfur by 43.48% with a TOF value that is relatively high, that is 183 h^{-1} (Table 3, Eq. (2)) and provides a conversion value ODS that is not much different from Indonesian commercial diesel, which is believed to contain many other compounds, not only DBT but thiophene and its derivatives and other compounds. Therefore, this catalyst has great potential by offering sufficient active sites and high reactivity for the ODS process. Consequently, it is deemed necessary to explore the course of the process further so that the collision of reactants on the catalyst surface is more effective and the type of reactor used so that it can increase conversion results.

Catalyst TOF

The TOF of the Fe-Co site on the catalyst assessed the reactivity of the catalyst site. The resulting TOF number was 183 h^{-1}. Measuring the TOF is a determining parameter for catalyst performance. TOF is the number of moles of reactant converted to the desired product by each active site per hour. This is calculated from the number of molecules converted as products in a certain period with the amount of metal embedded in the catalyst that functions as an active site (Eq. (2)), which

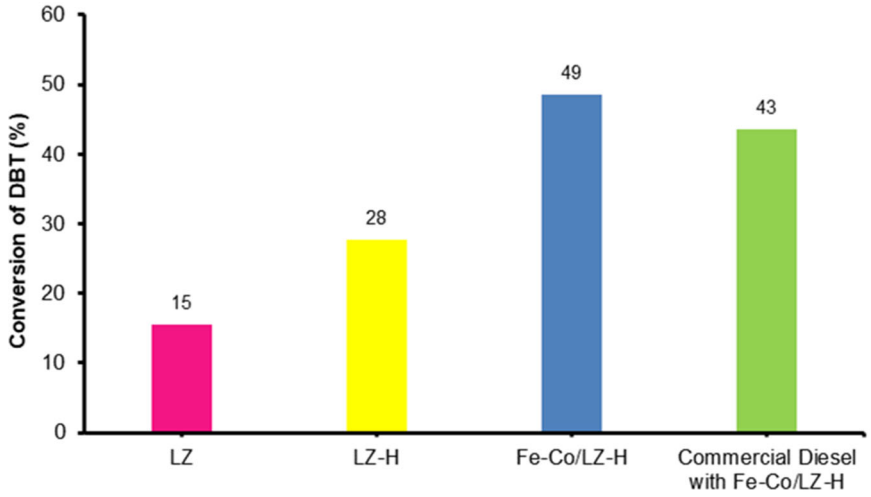

Fig 8. ODS model oil process with LZ, LZ-H, and Fe-Co/LZ-H catalysts, as well as ODS process for Indonesian commercial diesel with Fe-Co/LZ-H catalyst, under optimum conditions, i.e., the amount of catalyst as a dose of 2% (w/v), temperature 45 °C, time 45 min in 10 mL of fuel

can be said to directly measure the reaction productivity [14].

TOF is a measure of the intrinsic activity of a catalyst. It is an important parameter in catalyst science that measures the number of reactant molecules converted by one active site in a catalyst per certain unit of time. The TOF value is used to determine the efficiency and performance of catalysts in various reactions by providing an overview of the reaction speed at the molecular level in the catalyst's active site. This is important to understand because TOF can provide insight into how quickly a catalyst can catalyze a particular reaction, which influences the overall efficiency of the catalysis process [14]. TOF states that the amount of metal dispersed on the catalyst surface is sufficient as an active site capable of facilitating the desired product molecule by suppressing side reaction pathways [14,40].

Table 3 compares TOF numbers using a similar ODS method and without a mass transfer agent. Table 3 shows that the Fe-Co/LZ-H catalyst has a higher TOF number in the DBT process in the long-chain oil model, with the use of oxidant according to its stoichiometry, without any additional mass transfer agent or extractant. The operating conditions are mild, and the conversion results are close to the Indonesian commercial diesel ODS, which contains not only DBT but also thiophene compounds and their derivatives, as well as possibly other compounds. This means that the Fe-Co/LZ-H catalyst has the potential to continue to be explored to produce higher activity. The recommendation for this research is to continue exploring the reaction pathway for the ODS process with the Fe-Co/LZ-H catalyst, which will become a reference for work procedures used in the future, as well as exploring the type of reactor used.

Proposed reaction mechanism

This proposal is based on observations of the phenomena that occurred during the research so that further research can be carried out later. The Fe-Co/LZ-H structure requires a slightly different catalytic pathway than that commonly reported for ODS DBT, as shown in Fig. 9. The Fe-Co/LZ-H catalyst provides a different desulfurization system and solves the steric and biphasic problem. The Fe-Co/LZ-H catalyst is known to be hydrophobic, so it can be well dispersed with DBT in model oils that do not cause biphasic hindrance [6,10]. With hierarchical pores dominated by mesopores, it is easier to disperse so that DBT molecules can easily enter the catalyst pores because the steric barrier, which is a problem due to the large size of the organosulfur molecules in the fuel, has been overcome [10,14].

This distributed reaction of approximately 5 min is illustrated in Fig. 9 as R1 (reaction 1), which does not yet produce reaction energy. Still, the ferromagnetic properties of the Fe-Co species can overcome the resonance of the DBT organosulfur compound so that the DBT compound can be optimized in a position ready to accept electrons by releasing hydrogen atoms. Fe-Co species also readily accept and decompose H_2O_2. Then, H_2O_2 is added when the reactor conditions have reached the optimum temperature of 45°. The possible decomposition of H_2O_2 by Fe-Co active sites on the catalyst surface is shown in Scheme 2 [38,42].

Nie et al. [43] discovered that the mixed metal Fe-Co, a magnetic transition, exhibits potent oxidation activity in its oxide form, which has rarely been reported. When combined with the oxidant H_2O_2, the mixed metal oxide Fe-Co exhibits excellent synergy in oxidation activity, acting as a powerful peroxidase. This performance

Table 3. Comparison of reported TOFs of different catalysts

DBT in (model oil)	Catalyst	[O]/[S]	Condition	TOF (h^{-1})	Conv. of DBT (%)	Ref
n-octane	Amide-assisted- Ti $(OH_2)_2(OH)_2(OSi)_2$-Zeolites (AM-TS-95)	4.0 (TBHP)	60 °C 30 min	134.8	100.0 (initial concentration 300 ppm)	[14]
-	Co@C/P-5	7.5 (H_2O_2)	60 °C 60 min	104.0	89.0 -	[41]
n-hexadecane	Fe-Co/LZ-H	2.0 (H_2O_2)	45 °C 45 min	183.0	48.5 (initial concentration 500 ppm)	This work

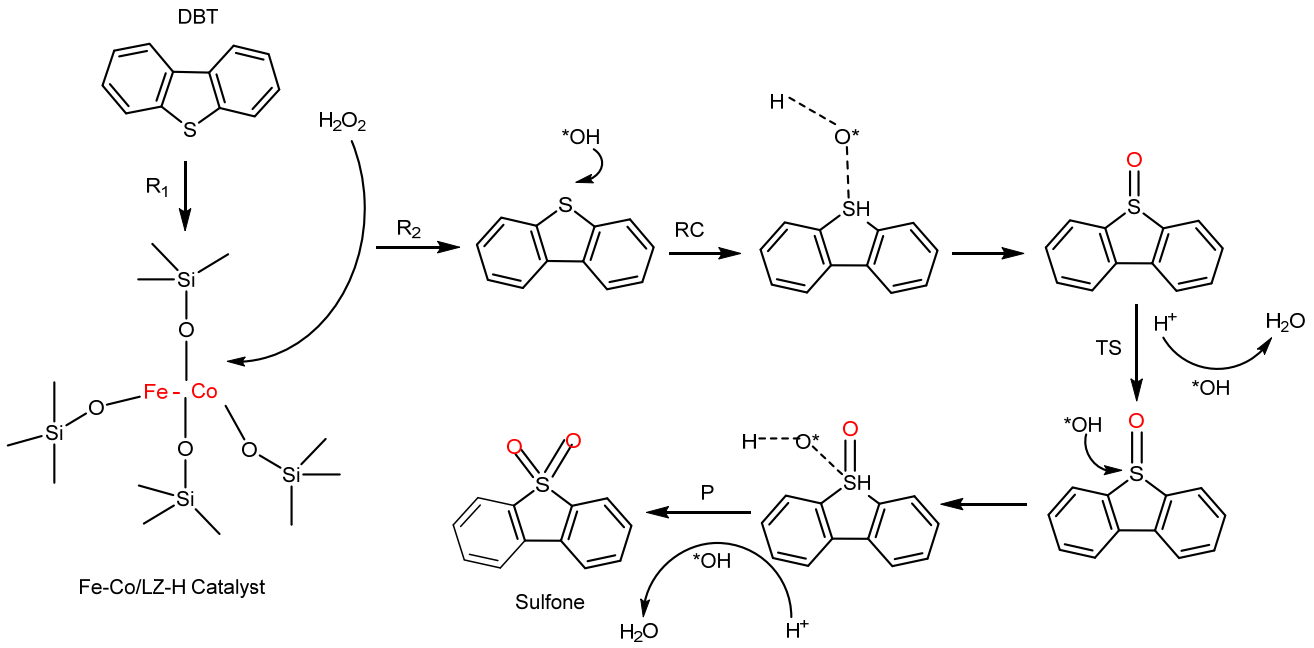

Fig 9. Proposed reaction mechanism of the ODS process with Fe-Co/LZ-H catalyst

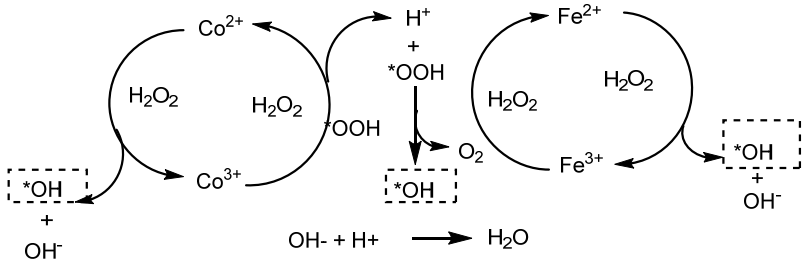

Scheme 2. Mechanism of the H_2O_2 decomposition reaction by the active site of the Fe-Co/LZ-H catalyst

is comparable to nano peroxidase enzymes that catalyze the oxidation of various organic substances using H_2O_2 [43]. The mixed metal oxide Fe-Co contributes to the Fenton-like reaction during the decomposition of H_2O_2, generating hydroxyl (*OH), and hydroperoxyl (*HOO). The Fenton reaction is an electrochemical process that transfers electrons between solid and liquid substances. The redox cycles of species Fe^{3+}/Fe^{2+} and Co^{3+}/Co^{2+} promote the continuous formation of *OH radicals [44-45], as illustrated by Scheme 2.

In Scheme 2, there are likely three potential pathways for generating *OH radicals. The bimetal Fe-Co present in LZ-H takes the form of either its oxide or mixed metal oxide. Co^{2+} contributes electrons to H_2O_2, catalyzing its decomposition and creating *OH radicals and HO^- ions. Hydrolysis occurs between Co^{3+} and H_2O_2, leading to the reduction of Co^{3+} to Co^{2+} and the production of *OOH radicals. Hydrolysis occurs between Fe^{3+} and H_2O_2, leading to the creation of hydroperoxyl *OOH, followed by the reduction of Fe^{2+} to create *OH. Through bimolecular reactions that release oxygen, *OOH radicals can generate *OH radicals [45].

In Fig. 9, the second reaction (R2) illustrates how the catalyst surface decomposes H_2O_2 into HO* and HOO*. These *OHs are crucial in oxidizing sulfur (S) in the DBT compound. This process involves *O binding to the S species, releasing H^+ (RC). Subsequently, H^+ reacts with *OOH to produce H_2O and hydroxyl *OH, which oxidizes the sulfoxide to sulfone (TS). The proposed reaction mechanism for the decomposition of H_2O_2 on the Fe-Co surface can generate enough HO* to

achieve sulfone yield (P). Fe-Co/LZ-H then returns to its initial state, characterized by its porous and hydrophobic framework, which helps contain the sulfone product and water and facilitates the separation of the resulting sulfone by decantation.

The energy profile resulting from the reaction path proposed and optimized with DFT calculation by the software is depicted in Fig. 10. DFT here is carried out by computer simulation using Gaussian09 software. DFT is a computational method used for chemical calculations, predicting electronic structures, complex spin transition properties, predicting the energy and geometry of compounds, reaction thermochemistry, vibrations, and the influence of isotopes on reaction mechanisms. Gaussian09 is a quantum chemistry program and solid-state physics software that is currently considered competent in this area [46]. DFT calculations are performed to obtain the benefits of more profound insight into the reaction mechanism of ODS to different active ingredients in a catalyst with information on the energy profile of each structure, which is optimized by a frequency model and optimization carried out by the software.

From Fig. 10, it can be seen that overall, the DBT oxidation at the Fe-Co/LZ-H site is exothermic, namely in the energy at the final reaction of -4.12×10^5 kJ mol^{-1} (P). Only in RC is the reaction endothermic, with an energy barrier of 4.69×10^4 kJ mol^{-1}, and this is easy to pass, thereby speeding up TS until it reaches the product [14]. This shows that the reaction easily occurs on the active site of Fe-Co/LZ-H. It is also known in theory that the ODS reaction occurs in two stages, namely the sulfoxide formation stage, followed by sulfone formation. This is one of the reasons why sulfone oxidation is often less successful. The sulfoxide formation stage is a nucleophilic event that requires electron transfer facilities from nucleophile species [47]. Even though, in theory, the oxidation reaction of organosulfur compounds is an electrophilic substitution reaction that involves electrophile species [48]. Here, Co is the responsible species for facilitating the formation of sulfoxide very quickly by removing the H atom from the organosulfur group and replacing it with oxygen from the *OH as a nucleophile

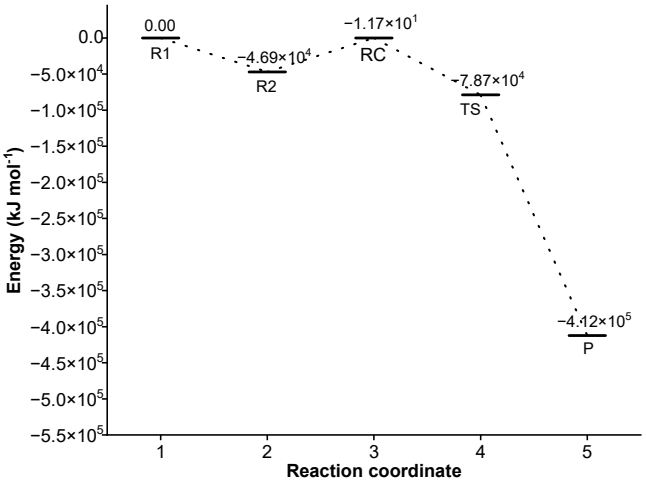

Fig 10. Energy profile of the ODS DBT reaction over the Fe-Co/LZ-H catalyst from the proposed reaction mechanism results from Gaussian 09 software simulation

species so that RC and TS are easily passed [49]. Electrophilic substitution towards P occurs easily in the presence of reactive oxygen as an electrophile species from the breakdown of *OOH is produced from the decomposition of H_2O_2 by Fe-Co. Fe strengthens the Fenton reaction in the decomposition of H_2O_2. HOO* is a molecule with one unpaired electron, so it is very reactive, and the presence of Fe-Co allows it to participate in reactions that produce electrophilic oxygen [42,50].

■ CONCLUSION

A new environmentally friendly catalyst, Fe-Co/LZ-H, has been obtained and characterized using BET, XRF, and contact angle methods. Its performance has been tested on model oil and Indonesian commercial diesel. Characterization shows the Fe-Co/LZ-H have hierarchical pores, namely micro, meso, and macropore, with dominated mesopore and high surface area. This is due to the unique catalyst manufacturing process, which involves a top-down dealumination method on the LZ catalyst support under reflux conditions. After impregnation with Fe-Co, the resulting excess mesopores remain to become Fe-Co/LZ-H. The catalyst performance is extraordinary, with a TOF number of 183 h^{-1} under operating conditions of 2% (w/v) catalyst

amount, temperature of 45 °C, [O]/[S] ratio of 2, and reaction time of 45 min. Additionally, the high Si/Al ratio of the catalyst provides hydrophobic properties, thereby increasing its effectiveness.

■ ACKNOWLEDGMENTS

The authors gratefully acknowledge financial support from the Universitas Bhayangkara Jakarta Raya for financial support and lab facilities, and the Directorate General of Higher Education (Ditjen Dikti) at the Indonesian Ministry of Education and Culture for supporting the 2023 PTUPT Grant.

■ CONFLICT OF INTEREST

The authors have no conflict of interest.

■ AUTHOR CONTRIBUTIONS

Lisa Adhani: original draft and formal analysis. Bambang Heru Susanto: supervision, review and editing. Mohammad Nasikin: methodology and supervision. All authors agreed to the final version of this manuscript.

■ REFERENCES

[1] Barker, J., Reid, J., Wilmot, E., Mulqueen, S., Angel Smith, S., Scurr, D., Snape, C., Kersting, R., Gauld, R., and Mulvey, R., 2020, Investigations of diesel injector deposits characterization and testing, *SAE Technical Paper 2020-01-2094*, https://doi.org/10.4271/2020-01-2094.

[2] Rajendran, A., Cui, T., Fan, H., Yang, Z., Feng, J., and Li, W., 2020, A comprehensive review on oxidative desulfurization catalysts targeting clean energy and environment, *J. Mater. Chem. A*, 85 (5), 2246–2285.

[3] Song, Y., Bai, J., Jiang, S., Yang, H., Yang, L., Wei, D., Bai, L., Wang, W., Liang, Y., and Chen, H., 2021, Co-Fe-Mo mixed metal oxides derived from layered double hydroxides for deep aerobic oxidative desulfurization, *Fuel*, 306, 121751.

[4] Jangi, F., Rahemi, N., and Allahyari, S., 2023, Oxidative desulfurization using nanocomposites of heterogeneous phosphotungstic acid over natural zeolites; optimization by central-composite design, *Pet. Sci. Technol.*, 41 (1), 104–122.

[5] Chen, L., and Yuan, Z.Y., 2022, Design strategies of supported metal-based catalysts for efficient oxidative desulfurization of fuel, *J. Ind. Eng. Chem.*, 108, 1–14.

[6] Wang, Y., Sun, C., Wang, R., Zhang, Z., Zhang, D., Zhang, Z., and Qiu, S., 2019, Preparation of amphiphilic Ti/ZSM-5 zeolite and its catalytic performance in oxidative desulfurization, *Chem. J. Chin. Univ.*, 40 (6), 1265–1270.

[7] Campos-Martin, J.M., and Capel-Sanchez, M.C., 2021, Catalytic oxidative desulfurization of liquid fuels, *ACS Symp. Ser.*, 1379, 143–174.

[8] Zhu, J., Wu, P., Chen, L., He, J., Wu, Y., Wang, C., Chao, Y., Lu, L., He, M., Zhu, W., and Li, H., 2020, 3D-printing of integrated spheres as a superior support of phosphotungstic acid for deep oxidative desulfurization of fuel, *J. Energy Chem.*, 45, 91–97.

[9] Wang, Y., Du, F., Wang, C., Zhao, J., Sun, H., and Sun, C., 2022, The synthesis and oxidation desulfurization performance of Ti-modified hierarchical cheese-like ZSM-5 zeolite, *J. Chem. Res.*, 46 (1), 17475198211068663.

[10] Zhu, Z., Ma, H., Liao, W., Tang, P., Yang, K., Su, T., Ren, W., and Lü, H., 2021, Insight into *tri*-coordinated aluminum dependent catalytic properties of dealuminated Y zeolites in oxidative desulfurization, *Appl. Catal., B*, 288, 120022.

[11] Jafarinasab, M., Akbari, A., Omidkhah, M., and Shakeri, M., 2020, An efficient Co-based metal-organic framework nanocrystal (Co-ZIF-67) for adsorptive desulfurization of dibenzothiophene: Impact of the preparation approach on structure tuning, *Energy Fuels*, 34 (10), 12779–12791.

[12] Jafarinasab, M., and Akbari, A., 2021, Co-ZIF-67 encapsulated phosphomolybdic acid as a hybrid catalyst for deep oxidative desulfurization, *J. Environ. Chem. Eng.*, 9 (6), 106472.

[13] Dashtpeyma, G., and Shabanian, S.R., 2023, Efficient photocatalytic oxidative desulfurization of liquid petroleum fuels under visible-light irradiation using a novel ternary heterogeneous $BiVO_4$-CuO/modified natural clinoptilolite zeolite,

J. Photochem. Photobiol., A, 445, 115024.

[14] Zhang, J., Bai, R., Feng, Z., and Li, J., 2024, Amide-assisted synthesis of TS-1 zeolites with active $Ti(OH_2)_2(OH)_2(OSi)_2$ sites toward efficient oxidative desulfurization, *Appl. Catal., B*, 342, 123339.

[15] Wardani, A.K., Ariono, D., Subagjo, S., and Wenten, I.G., 2019, Hydrophilic modification of polypropylene ultrafiltration membrane by air-assisted polydopamine coating, *Polym. Adv. Technol.*, 30 (4), 1148–1155.

[16] Qin, Z., Shen, W., Zhou, S., Shen, Y., Li, C., Zeng, P., and Shen, B., 2020, Defect-assisted mesopore formation during Y zeolite dealumination: The types of defect matter, *Microporous Mesoporous Mater.*, 303, 110248.

[17] Xue, Y., Niu, Y., Zheng, H., Cui, X., Ma, Q., Tang, J., and Ding, L., 2021, Selective dealumination of ZSM-5 by steaming and its effect on ethanol to propene, *J. Fuel Chem. Technol.*, 49 (8), 1111–1121.

[18] Aziz, I., Retnaningsih, T., Gustama, D., Saridewi, N., Adhani, L., and Dwiatmoko, A.A., 2021, Catalytic cracking of Jatropha oil into biofuel over hierarchical zeolite supported NiMo catalyst, *AIP Conf. Proc.*, 2349 (1), 020004.

[19] Beshtar, M., Khorasheh, F., Larimi, A., and Akbar Asgharinezhad, A., 2024, Photocatalytic oxidative desulfurization of model fuel using iron-molybdenum nanocatalyst based on cerium oxide (Fe_yMo_x/CeO_2) under visible light, *Fuel*, 360, 130549.

[20] Rachmawati, D.E., Susanto, B.H., and Nasikin, M., 2023, The effect of cerium promoted on Ni-Mo/Al_2O_3 in oxygen adsorption isotherm and oxidative desulfurization study, *AIP Conf. Proc.*, 2827 (1), 030029.

[21] Goodfellow, A.S., and Bühl, M., 2021, Hydricity of 3d transition metal complexes from density functional theory: A benchmarking study, *Molecules*, 26 (13), 4072.

[22] Hartmann, M., Thommes, M., and Schwieger, W., 2021, Hierarchically-ordered zeolites: A critical assessment, *Adv. Mater. Interfaces*, 8 (4), 2001841.

[23] Sihombing, J.L., Herlinawati, H., Pulungan, A.N., Simatupang, L., Rahayu, R., and Wibowo, A.A., 2023, Effective hydrodeoxygenation bio-oil via natural zeolite supported transition metal oxide catalyst, *Arabian J. Chem.*, 16 (6), 104707.

[24] Cieśla, J., Franus, W., Franus, M., Kedziora, K., Gluszczyk, J., Szerement, J., and Jozefaciuk, G., 2019, Environmental-friendly modifications of zeolite to increase its sorption and anion exchange properties, physicochemical studies of the modified materials, *Materials*, 12 (19), 3213.

[25] Osaki, T., 2018, Effect of sol–gel conditions on BET surface area, pore volume, mean pore radius, palladium dispersion, palladium particle size, and catalytic CO oxidation activity of Pd/Al_2O_3 cryogels, *J. Porous Mater.*, 25 (3), 697–711.

[26] Jia, X., Khan, W., Wu, Z., Choi, J., and Yip, A.C.K., 2019, Modern synthesis strategies for hierarchical zeolites: Bottom-up versus top-down strategies, *Adv. Powder Technol.*, 30 (3), 467–484.

[27] Schlumberger, C., and Thommes, M., 2021, Characterization of hierarchically ordered porous materials by physisorption and mercury porosimetry—A tutorial review, *Adv. Mater. Interfaces*, 8 (4), 2002181.

[28] Siauciunas, R., Smalakys, G., and Dambrauskas, T., 2021, Porosity of calcium silicate hydrates synthesized from natural rocks, *Materials*, 14 (19), 5592.

[29] Datar, A., Chung, Y.G., and Lin, L.C., 2020, Beyond the BET analysis: The surface area prediction of nanoporous materials using a machine learning method, *J. Phys. Chem. Lett.*, 11 (14), 5412–5417.

[30] Baekelant, W., Romolini, G., Sun, L., De Ras, M., Fron, E., Moreira, T., Viola, C., Ruivo, A., Laia, C.A.T., Martens, J., Martin, C., Kim, C.W., van der Auweraer, M., Roeffaers, M.B.J., Hofkens, J., and Coutino-Gonzalez, E., 2020, Tunable white emission of silver-sulfur-zeolites as single-phase LED phosphors, *Methods Appl. Fluoresc.*, 8 (2), 024004.

[31] Liu, K., and Ostadhassan, M., 2019, The impact of pore size distribution data presentation format on pore structure interpretation of shales, *Adv. Geo-Energy Res.*, 3 (2), 187–197.

[32] Qin, L., Niu, D., Li, N., Luo, X., Qin, X., Chen, J., Li, Y., and Shi, J., 2021, Hydrophobicity-induced electrostatic interfacial self-assembly for porous silica nanospheres with tunable pore sizes and pore hierarchies, *Chem. Eng. J.*, 405, 126936.

[33] Ding, L., Yue, X., Chen, Y., Wang, Z., Liu, J., Shi, Z., and Liang, Z., 2023, Tandem design of functional separators for Li metal batteries with long-term stability and high-rate capability, *Adv. Funct. Mater.*, 33 (43), 2304386.

[34] Sun, J., Fang, H., Ravikovitch, P.I., and Sholl, D.S., 2020, Understanding dealumination mechanisms in protonic and cationic zeolites, *J. Phys. Chem. C*, 124 (1), 668–676.

[35] Sun, Y., Lang, Q., Fu, G., Zhao, H., Dib, E., Liu, X., Yang, X., Lu, P., Yu, B., and Valtchev, V., 2024, Highly hydrophobic zeolite ZSM-8 with perfect framework structure obtained in a strongly acidic medium, *Microporous Mesoporous Mater.*, 363, 112839.

[36] Ismail, A., Saputri, L.N.M.Z., Dwiatmoko, A.A., Susanto, B.H., and Nasikin, M., 2021, A facile approach to synthesis of silica nanoparticles from silica sand and their application as superhydrophobic material, *J. Asian Ceram. Soc.*, 9 (2), 665–672.

[37] Alharbi, A.R., Alarifi, I.M., Khan, W.S., and Asmatulu, R., 2016, Highly hydrophilic electrospun polyacrylonitrile/polyvinypyrrolidone nanofibers incorporated with gentamicin as filter medium for dam water and wastewater treatment, *J. Membr. Sep. Technol.*, 5 (2), 38–56.

[38] Fang, Z., Zhao, Z., Li, N., Zhu, Z., Lu, W., Chen, F., and Chen, W., 2021, Low-temperature catalytic oxidative desulfurization by two-phase system with O-bridged diiron perfluorophthalocyanine, *Fuel*, 306, 121649.

[39] Nikmanesh, H., Jaberolansar, E., Kameli, P., Varzaneh, A.G., Mehrabi, M., and Rostami, M., 2022, Structural and magnetic properties of $CoFe_2O_4$ ferrite nanoparticles doped by gadolinium, *Nanotechnology*, 33 (4), 045704.

[40] Yunes, S., Kenvin, J., and Gil, A., 2023, On the genesis of a catalyst: A brief review with an experimental case study, *Eng*, 4 (3), 2375–2406.

[41] Bhadra, B.N., Mondol, M.M.H., and Jhung, S.H., 2024, Metallic cobalt-anchored carbon with non-metallic heteroatom decoration: Remarkably effective oxidative desulfurization catalyst, *Sep. Purif. Technol.*, 330, 125425.

[42] Wang, C., Ying, C., Tang, Y., Yan, Y., and Feng, X., 2020, Synergistic effect of Co(II) doping on FeS activating heterogeneous Fenton processes toward degradation of Rhodamine B, *Chem. Eng. J. Adv.*, 4, 100044.

[43] Nie, L., Li, S., Gao, X., Yuan, S., Dong, G., Tang, G., Song, D., Bu, L., and Zhou, Q., 2025, Sensitive visual detection of norfloxacin in water by smartphone assisted colorimetric method based on peroxidase-like active cobalt-doped Fe_3O_4 nanozyme, *J. Environ. Sci.*, 148, 198–209.

[44] Xue, C., Ma, J., Chen, X., Liu, D., and Huang, W., 2023, Efficient degradation of 2,4-dichlorophenol by heterogeneous electro-Fenton using bulk carbon aerogels modified in situ with FeCo-LDH as cathodes: Operational parameters and mechanism exploration, *J. Environ. Manage.*, 347, 119114.

[45] Zhang, J., Zhu, W., Li, H., Jiang, W., Jiang, Y., Huang, W., and Yan, Y., 2009, Deep oxidative desulfurization of fuels by Fenton-like reagent in ionic liquids, *Green Chem.*, 11 (11), 1801–1807.

[46] Ganesan, V., Mani, M.K., Narayanan, V., Shanmugasundram, E., Vellaisamy, K., Baskaralingam, V., Jeyaraj, J., Veerakanellore, G.B., Rajamohan, R., and Thambusamy, S., 2023, Synthesis, characterization of 4,4′-((1E,1′E)-hydrazine-1,2-diylidenebis(methanylylidene)) diphenol and the inclusion complex with γ-cyclodextrin as a fluorescent probe for detection of Al^{3+}, *J. Photochem. Photobiol., A*, 442, 114814.

[47] Sikarwar, P., Gosu, V., and Subbaramaiah, V., 2019, An overview of conventional and alternative technologies for the production of ultra-low-sulfur

fuels, *Rev. Chem. Eng.*, 35 (6), 669–705.

[48] Yahaya, A., and Abubakar, M., 2022, A review on desulfurization of kerosene using ionic liquids as catalysts, *Int. J. Sci. Global Sustainability*, 8 (2), 10.

[49] Sikarwar, P., Kumar, U.K.A., Gosu, V., and Subbaramaiah, V., 2018, Synergetic effect of cobalt-incorporated acid-activated GAC for adsorptive desulfurization of DBT under mild conditions, *J. Chem. Eng. Data*, 63 (8), 2975–2985.

[50] O'Day, P.A., Pattammattel, A., Aronstein, P., Leppert, V.J., and Forman, H.J., 2022, Iron speciation in respirable particulate matter and implications for human health, *Environ. Sci. Technol.*, 56 (11), 7006–7016.